ORIGINAL PAPER

Molecular dynamics study of Na$^+$ transportation in a cyclic peptide nanotube and its influences on water behaviors in the tube

Xuezeng Song · Jianfen Fan · Dongyan Liu · Hui Li · Rui Li

Abstract The dynamics of Na$^+$ transportation in a transmembrane cyclic peptide nanotube of 8×(WL)$_4$/POPE has been simulated. The curve of PMF (potential of mean force) for Na$^+$ moving through the tube, based on ABF (adaptive biasing force) method, indicates that Na$^+$ possesses lower free energy in an α-plane region than in a mid-plane one. It was found that Na$^+$ would desorb one or two water molecules in the first solvation shell when entering the tube and later maintain in a solvation state. The average numbers of water molecules around Na$^+$ are 4.50, 4.09 in the first solvation shell, and 3.10, 4.08 in the second one for Na$^+$ locating in an α-plane zone and a mid-plane region, respectively. However, water molecules far away from Na$^+$ location still nearly arrange in a form of 1-2-1-2 file. The dipole orientations of water molecules in the regions of gaps 1 and 7 display "D-defects", resulted from the simultaneous electrostatic potentials generated by Na$^+$ and the bare carbonyls at the tube mouths. Such "D-defects" accommodate the energetically favorable water orientations thereby.

Keywords Cyclic peptide nanotube · Molecular dynamics · Na$^+$ · PMF curve · Water chain

Introduction

Cyclic peptide nanotubes (CPNTs) are one class of artificial channels, being first synthesized by Ghadiri et al. in 1993. They are constructed by closed peptide rings with an even number of alternating D- and L-amino acid residues [1]. H-bonding interactions among peptide rings stabilize the tubular structure of a CPNT. The hydrophilic or hydrophobic characteristic of the outer surface makes a CPNT feasibly insert into a water solution or a lipid bilayer membrane [2–6]. With special structural characteristics, CPNTs are widely applied in the fields of biology, chemistry and materials [7, 8]. Being able to transport small species [9–13], they are widely used to mimic natural water and ion channels.

Engels et al. [14] first studied water transportation in a CPNT of 10×cyclo-[−(Gln-D-Ala-Glu-D-Ala-)$_4$], reporting a distinctive water chain arranging in 1-2-1-2 file, namely one water molecule in an α-plane zone (where a peptide subunit locates) and two in a mid-plane region (the zone between two adjacent peptide subunits). Subsequently, Tarek et al. [15] investigated the structural and dynamic properties of water transportation in a synthetic channel of 8×cyclo-[(L-Trp-D-Leu)$_3$-L-Gln-D-Leu] embedded in a fully hydrated DMPC bilayer, reporting that water molecules in the tube move in a concerted mode and are stabilized by forming H-bonds with the tube and other water molecules. García-Fandiño et al. [16] studied the transportation property of an α,γ-peptide nanotube and reported that the interior of the channel could form transient H-bonds with aqueous solvent, leading to a slow self-diffusion of water inside the tube. Fan et al. [9] studied the radial dependences of water chain structures, diffusion permeability (p_d) and osmotic one (p_f), based on the MD simulations of water transportation in three transmembrane CPNTs of 8×(WL)$_{n=3,4,5}$/POPE. Comparison of the correlations of channel-water movement in the three CPNTs suggests that water molecules form a typical single file in a hexa-CPNT, possess some cooperativity in a octa-CPNT with a nearly ideal 1-2-1-2 file of water chain and are completely chaotic in a deca-CPNT.

The earliest study of ion transportation in a CPNT was based on a self-assembled cylindrical β-sheet peptide architecture, which showed good channel-mediated ion-transport property with a rate of exceeding 10^7 ions per second [7].

X. Song · J. Fan (✉) · D. Liu · H. Li · R. Li
Faculty of Chemistry, Chemical Engineering and Materials
Science, Soochow University, Suzhou 215123,
People's Republic of China
e-mail: jffan@suda.edu.cn

J. Fan
e-mail: jffan1305@163.com

Asthagiri et al. presented a continuum and atomistic modeling of Li$^+$, Na$^+$, Rb$^+$ and Cl$^-$ partitioning into a self-assembled CPNT of $4 \times$ cyclo-[$-$(L-Ala-D-Ala)$_4$-] [17]. The PMF (potential of mean force) profiles for Na$^+$ and K$^+$ in a CPNT of $8 \times$-cyclo-[$-$(D-Ala-Glu-D-Ala-Gln)$_2$-], suggest that Na$^+$ has a longer residence time in the tube and a lower permeation than K$^+$ [18]. Subsequently, Dehez et al. [19] verified that the permeation of an ion channel depends not only on the characteristics of the tube, but also on the nature of the surrounding, based on the computation of the energetics of Na$^+$ transporting in a CPNT of $8 \times$cyclo-(LW)$_4$ immersed in a water medium and hydrated POPC bilayer, respectively. Choi et al. [20] calculated the free energies of Na$^+$, K$^+$ and Cl$^-$ ions permeating through a CPNT of $4 \times$ cyclo[$-$(D-Ala-Glu-D-Ala-Gln)$_2$-] by MD simulation, indicating that the CPNT has the selectivity to Na$^+$ and K$^+$.

When ions and water molecules coexist in a channel, they may influence each other. Hilder et al. found that the selectivity of a boron nitride nanotube to a cation or an anion is partly dependent on the unique structure of water inside the nanotube [21]. Yang et al. reported that water molecular asymmetry may produce frustrated orientations of water molecules, which was suggested as the source of cation selectivity of an electrically neutral but polar model channel [22]. The works of Furini et al. [23] and Saparov et al. [24] confirmed that the existence of K$^+$ can reduce the osmotic rate of water.

Although there are some reports about ion or water transportation in CPNTs, the influences of ions on water movement in CPNTs are not very clear. In this work, the PMF profile of a single Na$^+$ moving through a transmembrane CPNT of $8 \times$ (WL)$_4$/POPE was investigated in detail and the water-chain structures, dipole orientations of water molecules in the tube as a single Na$^+$ locating in a mid-plane region or an α-plane zone were analyzed.

Materials and methods

In this study, a self-programmed script was applied to construct a self-assembled cyclic octa-peptide nanotube of $8 \times$(WL)$_4$. Here, W and L represent the hydrophobic amino acid residues of tryptophan and leucine, respectively. The underlined letter corresponds to a *D*-amino acid residue.

1-palmitoy-2-oleoyl-sn-glycero-3-phosphoethanolamine (POPE) built with a plug of VMD software, was used as a bilayer lipid membrane. The energy-minimized octa-CPNT was embedded in a fully hydrated and balanced POPE membrane, ensuring the nanotube axis perpendicular to the plane of the lipid membrane. The overlapped phospholipid molecules were discarded to avoid poor van der Waals interactions. The center of the nanotube was coincided with that of the POPE membrane. Two water boxes, each with a length of 26 Å, were

added to the two sides of the system, respectively. A single Na$^+$ was put inside the CPNT, and one Cl$^-$ was introduced anywhere in the water boxes to ensure the whole system electrically neutral. Figure 1 depicts the configuration of the whole modeling system.

A CPNT embedded in a phospholipid membrane would inevitably incline to a certain degree [2, 3, 15]. In this work, harmonic potentials applied in x, y and z directions with a force constant (k) of 10 kcal (mol Å^2)$^{-1}$, respectively, were applied to the backbone C$_\alpha$ atoms of the nanotube to avoid channel inclination. Simulation process was investigated using a canonical NPT ensemble with periodic boundary conditions. The CHARMM27 [25] force field and TIP3P [26] water model were applied to describe the transmembrane nanotube and water molecules, respectively. Langevin dynamics was implemented to maintain the temperature of the system at 310 K, with a damping coefficient of 5/ps. Nosé-Hoover Langevin piston [27] method was used to control the system pressure at 1 bar by coupling in XY dimensions. The cycle of Langevin piston was 100 fs, with a decay time of 50 fs. Full electrostatic interactions were treated by the particle mesh Ewald (PME) approach [28]. The cut-off radii of long-range electrostatic and van der Waals interactions were set to be 12 Å, with a smoothing function applied from 10 Å. All the atomic initial velocities were set according to the Maxwell-Boltzmann distribution at 310 K. The final size of the whole system was $58 \times 58 \times 91.45$ Å, totally containing 31,472 atoms. The system was pre-equilibrated for 5 ns and further simulated for 10 ns with a time step of 1 fs. The trajectory was collected every 1 ps. The process of simulation was performed with the program NAMD 2.7 [29] and the results were analyzed with the molecular graphics program VMD 1.9 [30].

The potential of mean force (PMF) [31] of a single Na$^+$ along the CPNT axis was obtained by employing the adaptive biasing force (ABF) [32] method. The mean force exerted on Na$^+$ along a chosen reaction coordinate (ξ) was compensated by an equal and opposite biasing force, allowing Na$^+$ to move across the barriers and escape from the minima of the free energy surface. Here, ξ was defined as the separation between Na$^+$ and the center of the nanotube along the tube axis, ranging from -20 Å to 20 Å. With the purpose of enhancing the computational efficiency of the ABF algorithm, the whole span of the reaction coordinate (ξ) was subdivided into eight equally spaced windows, each with a width of 5 Å. First, a steered molecular dynamics (SMD) [33–35] simulation was carried out to pull Na$^+$ moving through the whole range of ξ. Then, a separate ABF simulation for each window was performed with the initial structure created from the above SMD trajectory. Each window was further divided into 50 bins with a width of 0.1 Å, which was sufficiently small to generate a smooth PMF profile. The first 1000 samples of each bin were discarded for the statistical analysis of data to avoid non-equilibrium effects of the kinetic system.
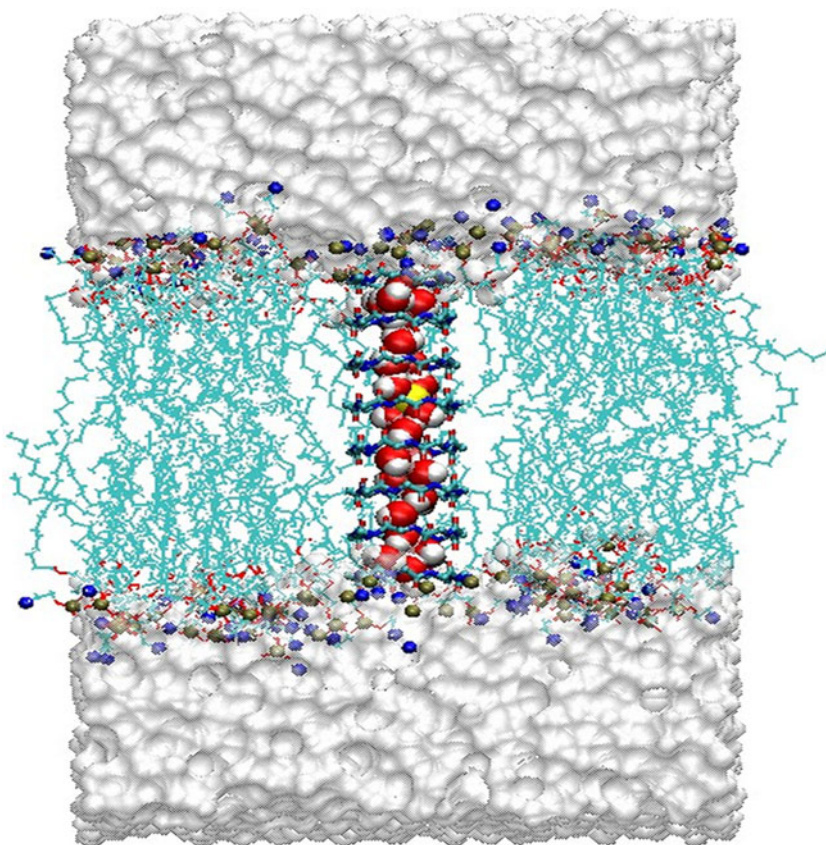
Results and discussion

Thermodynamic process of Na$^+$ transporting in the CPNT

The potential of mean force (PMF) of a single Na$^+$ along the
CPNT axis has been obtained by the ABF method and is
depicted in Fig. 2. Energy barriers at both ends of the channel
are much higher than those inside the tube, indicating that Na$^+$
is inclined to remain inside the tube. The PMF profile for Na$^+$
inside the tube fluctuates with barriers and wells in mid-plane
and α-plane regions, respectively. This is because the number
of water molecules around Na$^+$ locating in an α-plane zone is
more than that in a mid-plane region (see later section). Here,
the region near the plane of peptide C$_\alpha$ atoms is designated as
an α-plane zone and that between two adjacent α-plane zones
is defined as a mid-plane region [14]. The distance between
two adjacent energy barriers (or wells) is 4.8 Å, being consis-
tent with the gap distance between two adjacent peptide rings
[1, 3, 36]. The oscillation of the PMF curve reflects the
geometry of the cavity. Our PMF result is similar to that of
Dehez et al. [19], but somewhat different from that of Hwang
et al. [18, 20], with the lowest energy well in the middle of a
hydrophilic CPNT. It was speculated that such difference may
come from the different environments that CPNTs insert in. In
our work, a CPNT was embedded in a fully hydrated and

balanced POPE membrane. However, a CPNT was inserted in
a water solution in the work of Hwang's.

The total non-bonding interaction energy ($E_{total}^{non-bond}$) is
defined as

$$E_{total}^{non-bond} = E_{Na^+-water}^{elec} + E_{Na^+-tube}^{elec} + E_{Na^+-lipid}^{elec}$$
$$+ E_{Na^+-water}^{vdw} + E_{Na^+-tube}^{vdw} + E_{Na^+-lipid}^{vdw}. \quad (1)$$

The former three items donate the electrostatic interactions
of Na$^+$ with the channel-water, CPNT framework and lipids,
respectively. The latter three items represent the correspond-
ing van der Waals interactions. Each item was separately
investigated, based on a simulation of 1 ns with a time step
of 1 fs, in which a single Na$^+$ was put at the positions of $z=20$,
19, 18, … , −18, −19, −20 Å, respectively. The first 500 ps
was for equilibration and the data was collected for the last
500 ps. The results are illustrated in Fig. 3. The van der Waals
interactions of Na$^+$ with the tube and channel-water both
change little along the tube axis, and that between Na$^+$ and
the lipids is weak due to the long distances between them. The
fluctuation of the total non-bonding interaction energy is
mainly contributed by the sum of the electrostatic interaction
energies of Na$^+$ with the channel and water molecules in the
tube. Especially, the latter plays a determinant role. In the

Fig. 2 The PMF profile for a single Na$^+$ passing through the transmembrane CPNT of 8×(WL)$_4$/POPE along the tube axis (z). The region near the plane of peptide C$_\alpha$ atoms is designated as an α-plane zone and that between two adjacent α-plane zones is defined as a mid-plane region
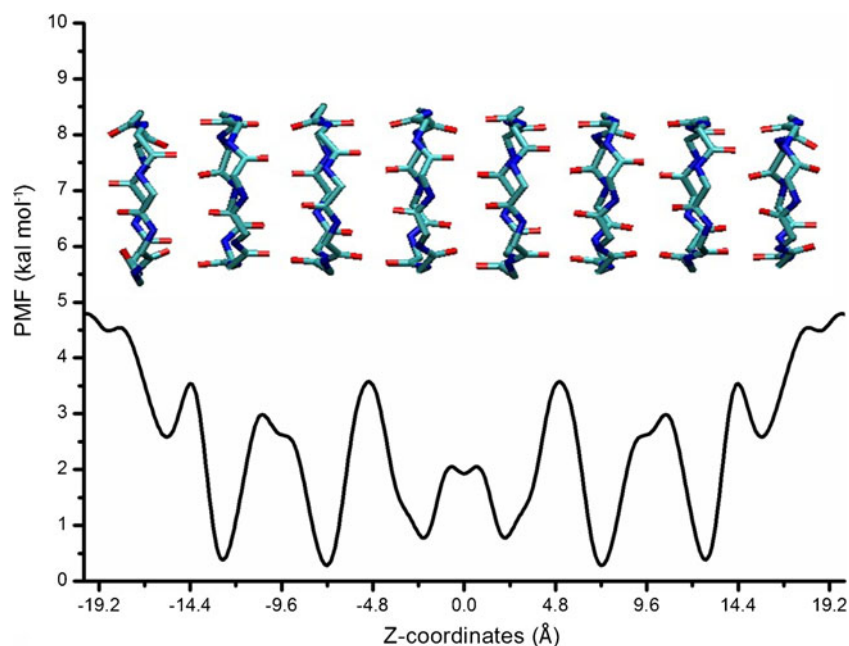
process of Na$^+$ entering the CPNT from water reservoir, the electrostatic interaction energy between Na$^+$ and the channel water is gradually weakened, while that between Na$^+$ and the tube becomes more strong. As a single Na$^+$ moving through the CPNT, the profiles for these two items both present wave-like patterns, but the trends are just the opposite.

The numbers of oxygen atoms of water molecules and carbonyl moieties coordinating with Na$^+$ are depicted in Fig. 4. In bulk, six water molecules [34] directly coordinate with Na$^+$ in the first solvation shell with a radius of 3.1 Å [37, 38]. As a single Na$^+$ enters the tube from bulk, the number of

water oxygen atoms changes from six (in bulk) to five (at the CPNT mouth) at first and then partly to four. One or two water molecules are removed from the first solvation shell of Na$^+$, presenting a desolvation process. Meanwhile, the carbonyl oxygen atoms of the CPNT backbone begin to interact with Na$^+$. In case of not enough surrounding water molecules in the tube due to the spatial restriction, such interaction is favorable to reduce the system energy. As a single Na$^+$ moves through the CPNT, water molecules are intermittently replaced by carbonyl groups to coordinate with Na$^+$. As described in Fig. 4, the number of water oxygen atoms in

Fig. 3 The electrostatic and vdW interaction energies of Na$^+$ with the channel, channel-water molecules and lipids along the tube axis (z). The total non-bond energy is also included. The vdW interaction energies of Na$^+$ with the channel, channel-water molecules and lipids are described with green, blue and magenta lines, respectively. Their electrostatic energies are described with red, black and cyan lines, respectively. The yellow line represents the profile of the total non-bonding interaction energy
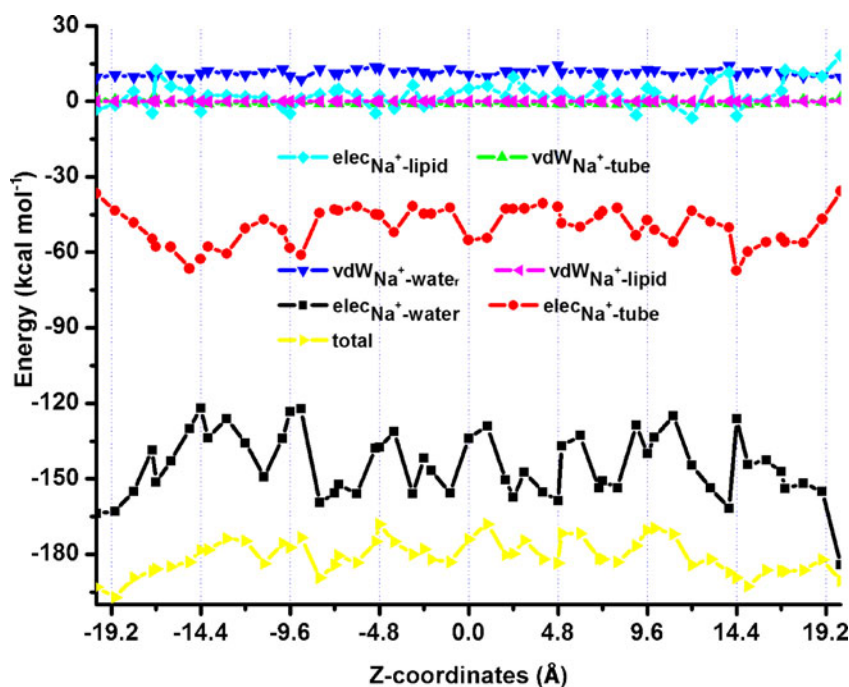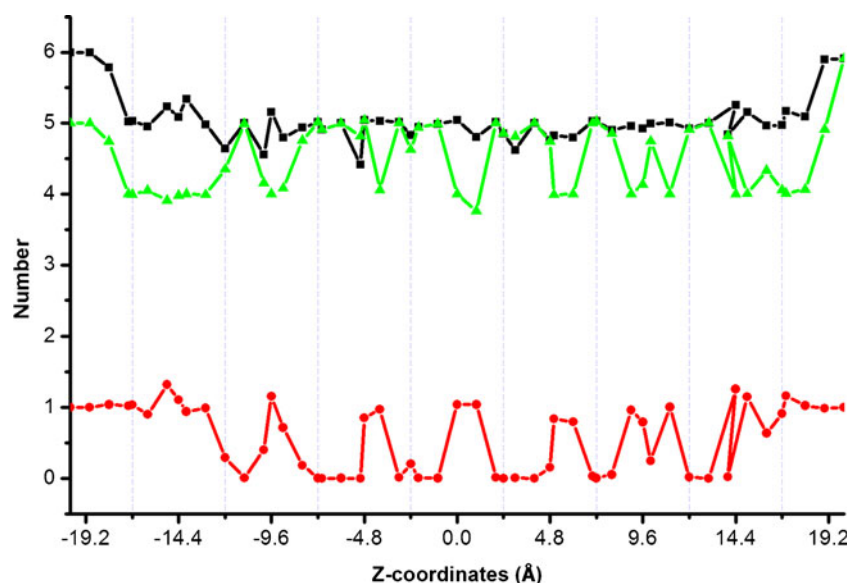
Fig. 4 The numbers of oxygen atoms of water molecules (*green line*) and carbonyl moieties (*red line*) coordinating with Na$^+$ along the tube axis (z). The sum of the two is also included, shown in a black line
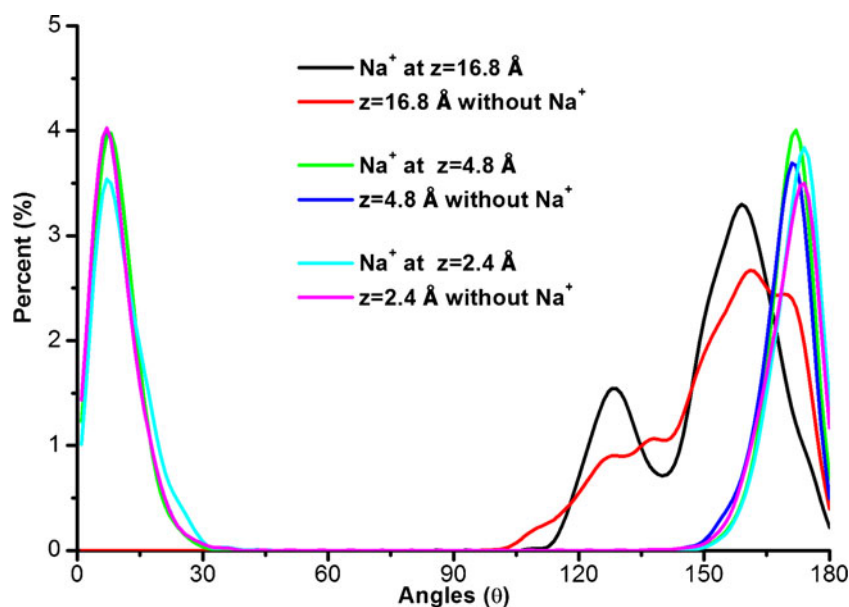

the first solvation shell of Na$^+$ is about four in a mid-plane region but about five in an α-plane zone. Obviously, when Na$^+$ locates in a mid-plane region, fewer neighboring water molecules are available in its neighboring α-plane zones.

In order to clarify the influences of the introduction of Na$^+$ in a CPNT on the orientations of the backbone carbonyl groups, the distribution of the angles (θ) between the vectors (from O to C) of carbonyl groups and the tube axis (z) has been investigated. Here, θ is defined as

$$\theta = a\cos\left(\frac{\overrightarrow{r}_{oc}\cdot\widehat{z}}{\left|\overrightarrow{r}_{oc}\right|\left|\widehat{z}\right|}\right), \qquad (2)$$

where $\overrightarrow{r}_{oc} = \overrightarrow{r}_o - \overrightarrow{r}_c$, and $\widehat{z}$ is a unit vector parallel to the nanotube axis (z). Eight carbonyl groups near Na$^+$ were

selected to calculate the angle (θ) distribution. Simulations were performed for a single Na$^+$ typically introduced at the positions of $z=2.4$, 4.8 and 16.8 Å, corresponding to an α-plane zone, a mid-plane region and the mouth of the tube, respectively. For comparison, similar simulations were also performed for the cases without Na$^+$. The results are depicted in Fig. 5. It can be found that four curves for Na$^+$ locating at $z=2.4$ Å (an α-plane zone), $z=4.8$ Å (a mid-plane region) and the corresponding cases without Na$^+$ have similar profiles, all showing two peaks around $\theta=10°$ and $\theta=170°$. These two angles indicate that most carbonyl groups thereby participate in the H-bonding network between neighboring peptide subunits by orienting near to the positive or negative directions of z-axis. The two curves for Na$^+$ locating at $z=16.8$ Å (an α-plane near the CPNT mouth) and the case without Na$^+$ show significant difference. The peak at

Fig. 5 The angle (θ) distributions of eight backbone carbonyl groups around Na$^+$ locating in a mid-plane region, an α-plane zone and at the entrance of the CPNT, corresponding to 2.4, 4.8 and 16.8 Å of z coordinates, described with cyan, green and black lines, respectively. For comparison, the results for the cases without Na$^+$ are also included and described with magenta, blue and red lines, respectively
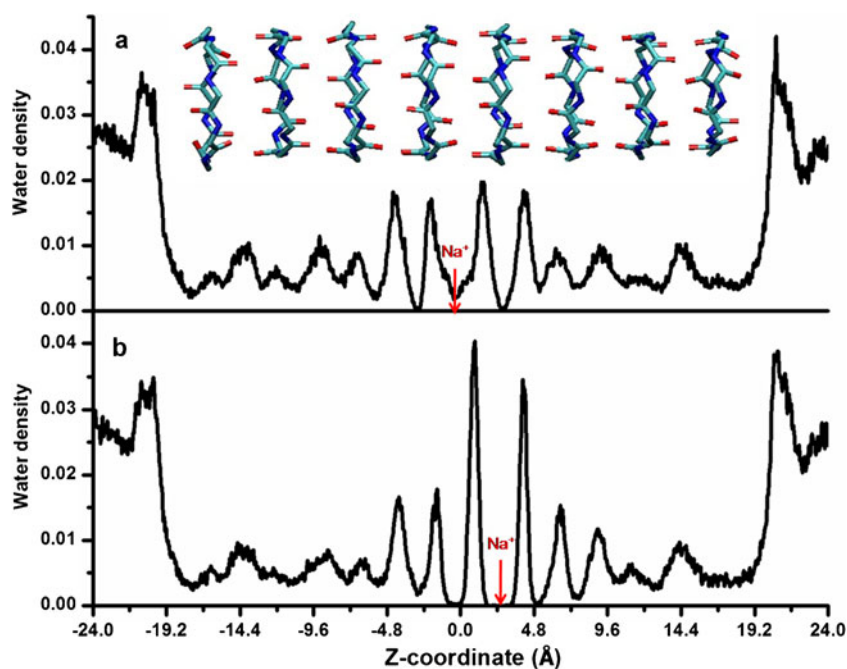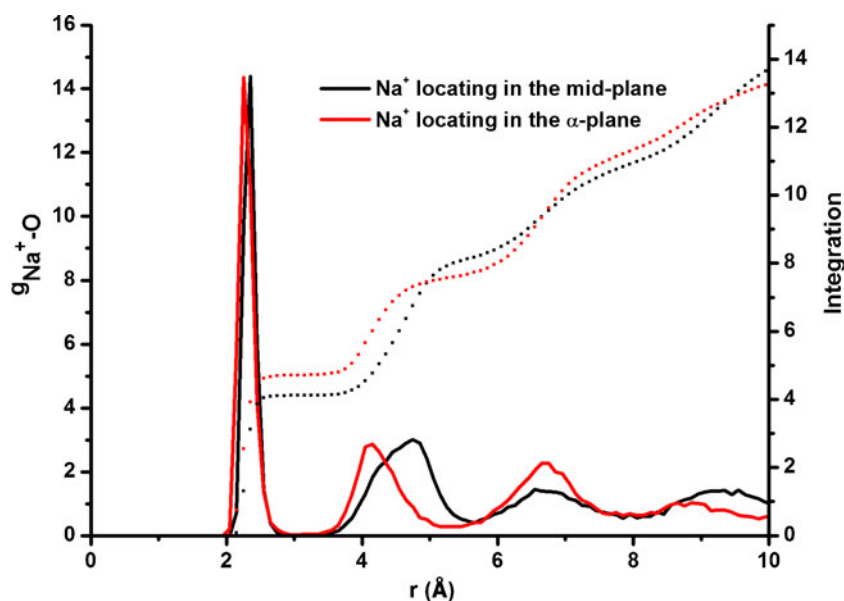
θ=130° infers that the strong electrostatic interaction between the carbonyl oxygen atoms near the CPNT mouth and Na$^+$ distinctly changes the orientations of the carbonyl moieties. It can be speculated that the reason why a CPNT has a selectivity for cations is closely related to such electrostatic interaction. When a cation such as Na$^+$ approaches to a CPNT mouth from bulk aqueous solution, one or two water molecules are removed from the first solvation shell. At the same time, carbonyl oxygen atoms replace water oxygen ones to coordinate with Na$^+$, which is in favor of reducing the energy of the whole system. However, for Cl$^-$, an anion, the repulsive interaction between it and the bare carbonyls at a CPNT mouth may push it outside of the channel.

Influences of Na$^+$ on water structure in the CPNT

The incorporation of Na$^+$ in a CPNT would inevitably influence the water movement in the channel. Figure 6 shows the probability density profiles of water molecules along the axis of the CPNT. The two curves both show certain symmetry on both sides of Na$^+$. It can be found that four high peaks arise around Na$^+$ locating in the mid-plane region of gap 4, and two high peaks and four middle ones around Na$^+$ locating in the α-plane zone between gaps 4 and 5. In the region far away from Na$^+$, strong peaks in mid-plane regions ($z=\pm 14.4$ Å, ± 9.6 Å) and weak peaks in α-plane zones ($z=\pm 16.8$ Å, ± 7.2 Å) occur in turn. It is worth noting that the peaks around the location of

Fig. 7 The radial distribution
function (RDF) of g_{Na^+-O}
between Na$^+$ and water oxygen
atoms when a single Na$^+$
locating in the mid-plane region
of gap 4 (solid black line) and in
the α-plane zone between gaps
4 and 5 (solid red line),
respectively. The integration
curves of the RDF profiles are
also included and shown in
dotted black and red lines,
respectively

Na^+ are much higher than others. The reason is that the collected samples there are probably much more than those in other regions, due to the strong electrostatic interactions between water molecules and Na^+.

In order to further understand the distribution of water molecules in the tube, the radial distribution functions (RDFs) between different species were computed. When a particle moves through a CPNT, 1-D RDF may be more indicative. The conventional definition of RDF for a three-dimensional isotropic system cannot effectively describe the detailed structures of particles in a channel such as a CPNT at large range. To overcome this limitation, a revised form of RDF, defined as [11]

$$g(r) = \frac{\langle \Delta N \rangle}{2A\rho\Delta r} = \frac{\langle \Delta N \rangle}{2\langle N \rangle \Delta r} L \tag{3}$$

was applied, where A is the cross-sectional area of a CPNT normal to the channel axis, L is the total length of the CPNT and $\langle N \rangle$ is the average number of water molecules in the CPNT. The results of $g_{Na^+\text{-}O}$ between Na^+ and channel water oxygen atoms when a single Na^+ locating in the mid-plane region of gap 4 and in the α-plane zone between gaps 4 and 5, respectively, were depicted in Fig. 7. The integrations of $g_{Na^+\text{-}O}$ profiles in Fig. 7 indicate that a little more water molecules locate in the first solvation shell of Na^+ and less in the second one when Na^+ locates in an α-plane zone.

Fig. 8 The structures of water chains inside the transmembrane CPNT of 8×(WL)$_4$/POPE for a single Na^+ locating in the α-plane zone between gaps 4 and 5 (*right*) and in the mid-plane region of gap 4 (*left*), respectively. In the region far away from Na^+, water molecules nearly arrange in a form of 1-2-1-2 file. Na^+, water oxygen atoms, water hydrogen atoms are represented in vdW spheres and colored yellow, red and white, respectively
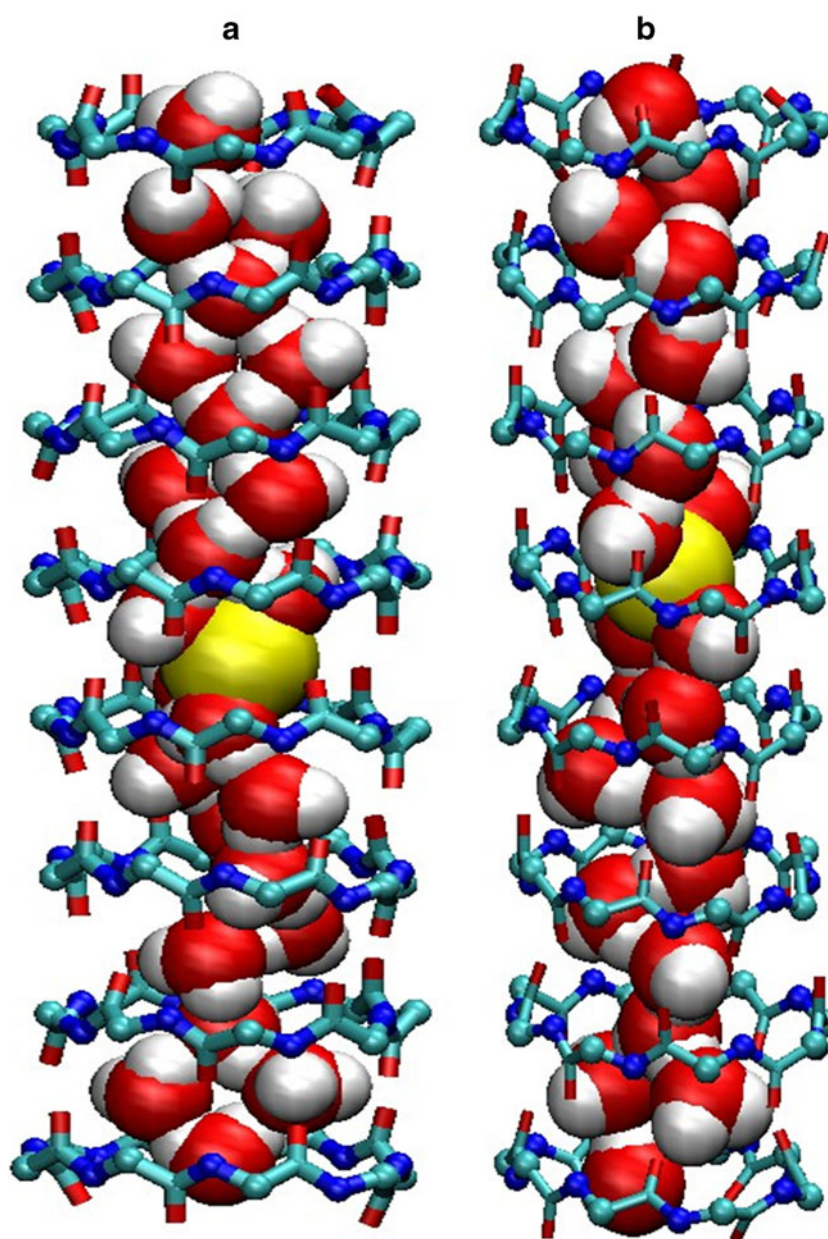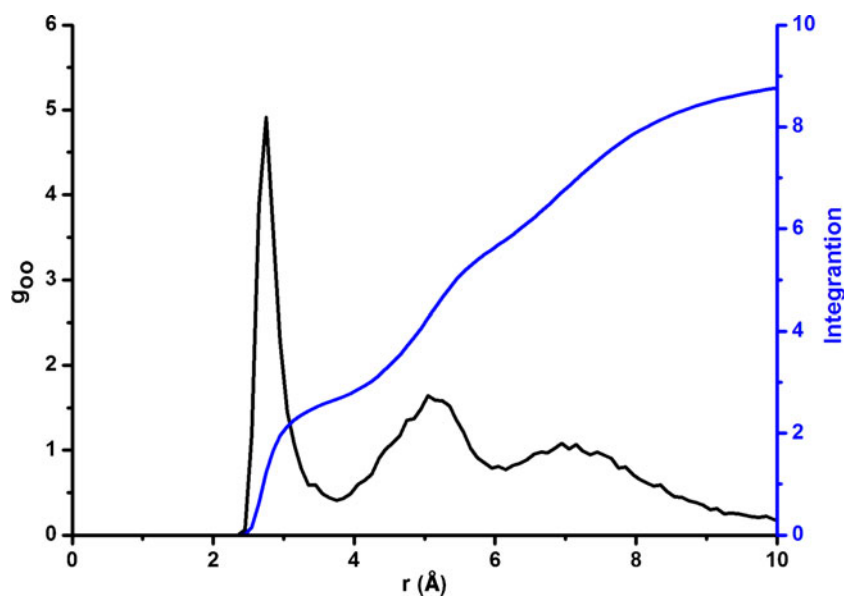
Fig. 9 The radial distribution function (RDF) of g_{oo} between water oxygen atoms in the region away from the Na^+ location (in *black*) and the corresponding integration curve (in *blue*)

Among the total 1802 frames for a single Na^+ locating in an α-plane, there are 940, 841 and 21 frames associated with four, five and six water molecules in the first solvation shell of Na^+, respectively. And the results are 1467, 317 and 18 frames, respectively, for Na^+ locating in a mid-plane region. Primarily, four or five water molecules may be in the first solvation shell of Na^+. The ratio between the two cases is approximately 1.1:1 for Na^+ in an α-plane zone, but 4.6:1 for Na^+ in a mid-plane region. Thereby, the numbers of water molecules in the first solvation of Na^+ are 4.50 ($=4\times1.1/2.1+5\times1/2.1$) for Na^+ in an α-plane zone and 4.09 ($=4\times4.6/5.6+5\times1/5.6$) for Na^+ in a mid-plane region, respectively. The results are consistent with the integrations of g_{Na^+-O} profiles in Fig. 7. Also, it can be found that the numbers of water molecules in the second solvation shell of Na^+ are 3.10 and 4.08 for Na^+ locating in an α-plane zone and in a mid-plane region, respectively.

In the region far away from Na^+ location, water molecules nearly arrange in 1-2-1-2 file as shown in Fig. 8. The RDF of g_{oo} between the oxygen atoms of these water molecules is shown in Fig. 9. The sharp and high peak at 2.8 Å suggests that most neighboring water oxygen atoms are separated by nearly the same distance. Its integration up to the limit of the distance between water oxygen atoms of 3.75 Å gives an average value of 2.85 water molecules in the first solvation shell. The second peak of g_{oo}, much lower and broader than the first one, ranges from 3.75 to 6.05 Å. The integration of the second peak gives a value of 3.14 water molecules in the second solvation shell. In the case without Na^+, the unique steric constraints of the transmembrane CPNT of $8\times$-cyclo-$(WL)_4$/POPE results in a distinguished wavelike pattern of water chain, arraying in a form of 1-2-1-2 file. The ideal values of the average numbers of water molecules in the first

Fig. 10 The average values of the angles (θ) between water molecular dipoles and the z-axis of the transmembrane CPNT of $8\times(W\underline{L})_4$/POPE in individual gaps when a single Na^+ was put in the mid-plane region of gap 4 (*black line*) and in the α-plane zone between gaps 4 and 5 (*red line*), respectively. The error bars are shown as vertical lines
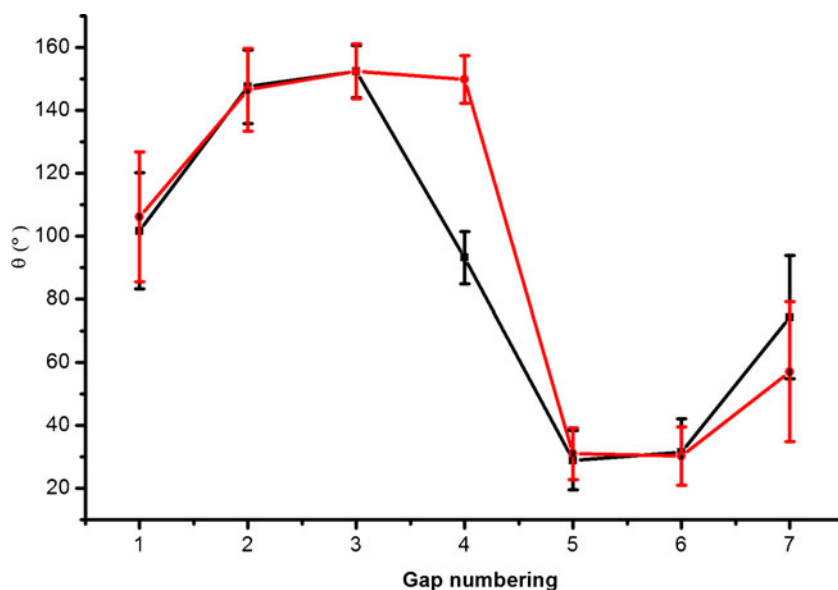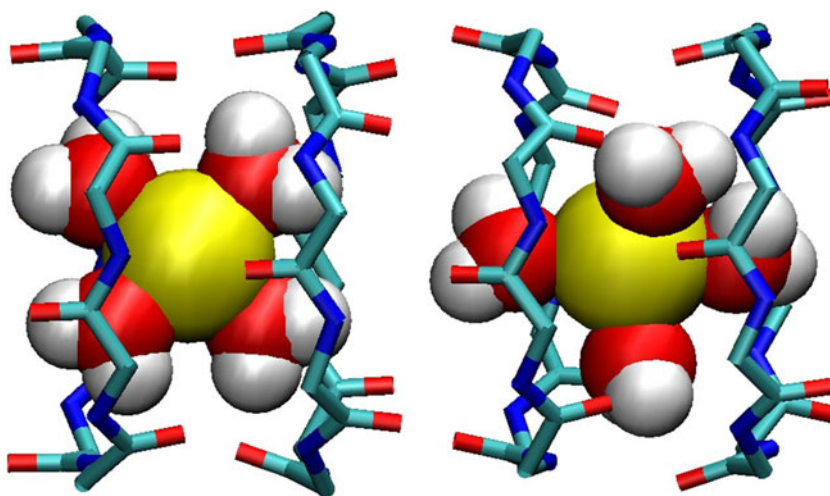
and second solvation shell are both 3.3 [11]. Therefore, the introduction of Na$^+$ exerts slight influence on the structure of water chain in the region far away from Na$^+$, where water molecules arrange nearly in a form of 1-2-1-2 file.

Influences of Na$^+$ on water dipole orientations in the CPNT

The dipole orientation of water chain in a nanotube would be inevitably affected by the incorporation of Na$^+$ in the channel. The dipole orientation of a water molecule is defined from the oxygen atom to the geometric center of the two H atoms. A single Na$^+$ was introduced in the mid-plane region of gap 4 or in the α-plane zone between gaps 4 and 5. Angles (θ) between the dipole orientations of water molecules and z-axis (the channel axis) have been investigated based on a 10 ns MD trajectory. The average results in individual gaps are described in Fig. 10. Obviously, the average values of the angles (θ) in gaps 1, 2 and 3 are much greater than 90° regardless of the

location of Na$^+$. Conversely, those in gaps 5, 6 and 7 are less than 90°. It is worth noting that the mean value of the angles (θ) in gap 4 approaches 90°, with Na$^+$ locating in gap 4. This is resulted from the diagonal distribution of water molecules around Na$^+$, shown in Fig. 11.

In order to further investigate the dipole orientations of water molecules in the channel, the order parameter (P) of water molecular dipole orientations has been calculated, which is defined as

$$P = \left(3 < \cos^2\theta > -1\right)/2. \tag{4}$$

The values of P, ranging from 1.0 to 0.0, reveal that the dipole orientations change from a complete order to a complete disorder. A negative value means that water molecular dipole orientation tends to be perpendicular to a tube axis. The order parameters (P) of the dipole orientations of water molecules in individual gaps with Na$^+$ locating in the mid-

Fig. 12 The order parameters (P) of the water dipole orientations in individual gaps with a single Na$^+$ locating in the mid-plane region of gap 4 (black line) and in the α-plane zone between gaps 4 and 5 (red line), respectively
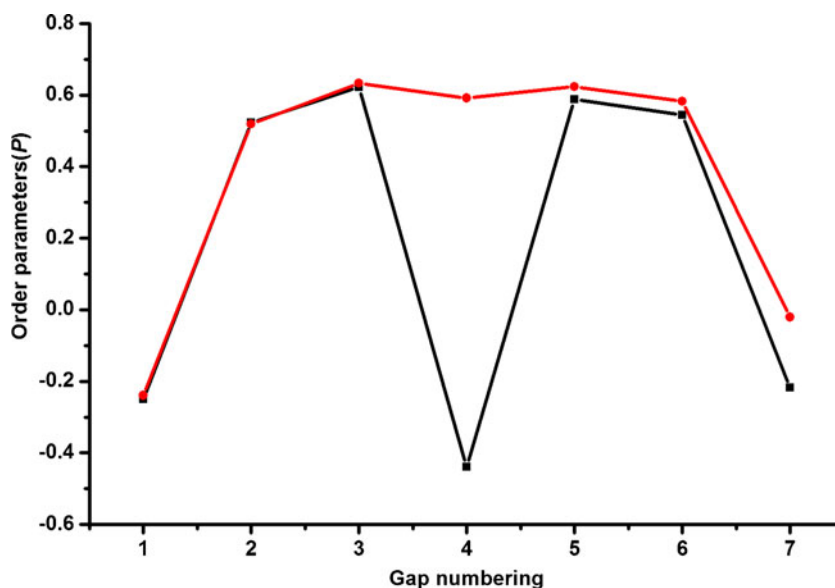
Fig. 13 The distributions of angles (θ) between water molecular orientations and the z-axis of 8×(WL)$_4$/POPE in individual gaps when a single Na$^+$ locates in the α-plane zone between gaps 4 and 5 (**a**) and in the mid-plane region of gap 4 (**b**), respectively. The result when a single Cl$^-$ was introduced in the mid-plane region of gap 4 is illustrated in the partial image (**c**). The distributions of angles (θ) in gaps 1, 2, … , 6, 7 are described with black, red, green, blue, cyan, magenta and yellow lines, respectively
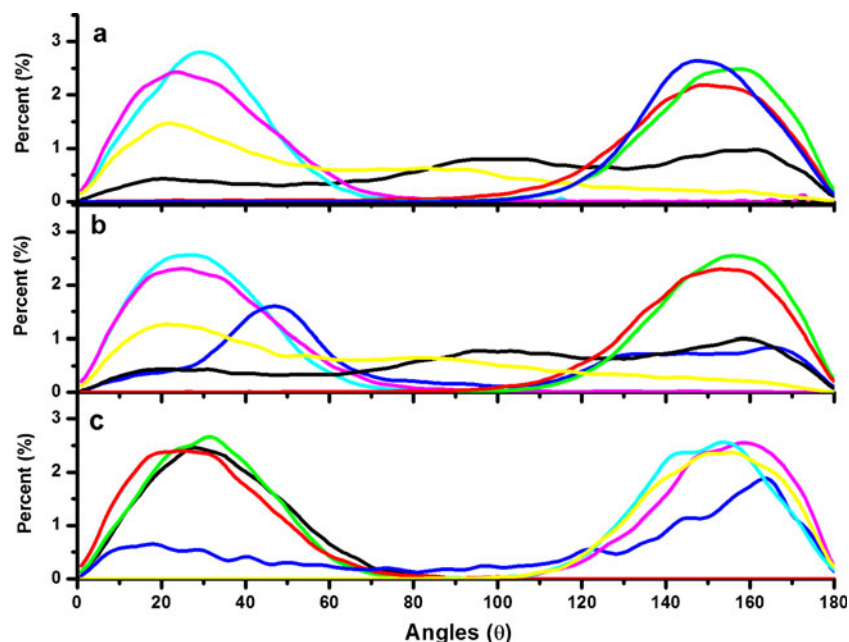

plane region of gap 4 and in the α-plane zone between gaps 4 and 5 have been computed and are depicted in Fig. 12, respectively. The two curves both describe that the values of P are all positive in gaps 2, 3, 5 and 6, indicating that the water molecular dipoles in these gaps are much more orientated. The negative values of P in gaps 1 and 7 indicate the dipole orientations of water molecules in these regions tend to be perpendicular to the tube axis.

The distributions of the angles (θ) in individual gaps are described in Fig. 13. It is clear that whether Na$^+$ locates in the

α-plane zone between gaps 4 and 5 (Fig. 13a) or in the mid-plane region of gap 4 (Fig. 13b), the curves in gaps 2, 3, 5 and 6 all present strong peaks in the range of 10~40° or 140~170° of the angles (θ). While those in gaps 1 and 7 near the two ends of the CPNT show weaker peaks in these regions, together with broad peaks around 90° of the angles (θ). This phenomenon indicates that the dipole orientations of water molecules in gaps 2, 3, 5 and 6 are mainly determined by the incorporation of Na$^+$. The electrostatic interactions between Na$^+$ and water molecules result that the dipole

Fig. 14 The schematic diagrams of a "D-defect" and "L-defect" in a water chain (**a**) and the "D-defect" in water chain in the transmembrane CPNT of 8×(WL)$_4$/POPE with a single Na$^+$ in the middle of the tube (**b**). Here illustrated is only half of the tube
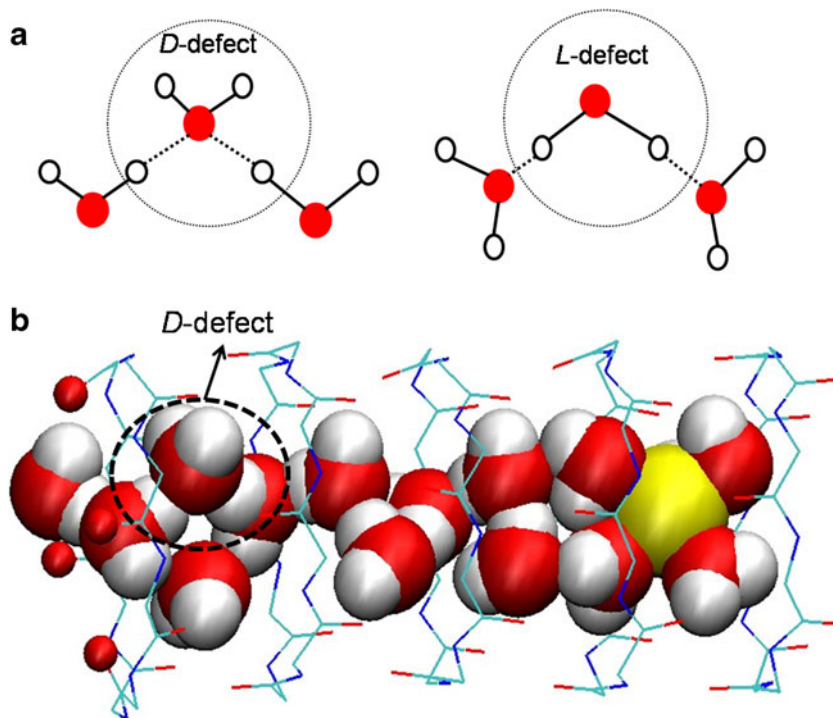
orientations of water molecules in these regions all point to the opposite of Na^+ location. Therefore, water molecules in gaps 1, 2 and 3 possess θ>90, while those in gaps 5, 6 and 7 have θ<90 when Na^+ locates in the middle of the channel.

Owing to dipole-dipole interactions, water molecules inside a nanotube maintain concerted dipole orientations [39]. Namely, water molecules in a nanochannel tend to form a water chain with the same dipole orientations, either upward or downward. In a flawless H-bond network, all the dipoles of water molecules point to the same direction. When the dipole orientations of a water chain at the two ends of a channel point to the opposite directions, there would be a H-bond defect associated with the network, indicated by the peak at 90° of the angle (θ). Usually, two kinds of H-bond defects may occur in a water chain, shown in Fig. 14a. In a "L-defect" [40, 41], a water molecule acts as a H-bond donor to its two neighboring water molecules. While in a "D-defect", it serves as a H-bond receptor. Only "D-defects" were observed in this system, occurring in gaps 1 and 7. When Na^+ locates inside a CPNT, channel-water molecules suffer two kinds of orientation effects. One comes from positive Na^+, resulting that the dipole orientations of channel-water molecules point to the opposite of Na^+ (i.e., pointing to an end of a CPNT). Another comes from the negative carbonyl groups at the two mouths of a CPNT. As shown in Fig.14b, the electrostatic interactions from the carbonyl oxygen atoms (represented in red vdW spheres) at a channel mouth attract the neighboring water H atoms to face the negative carbonyl oxygen atoms, resulting that the dipole of this neighboring water points to the middle of the CPNT. Due to dipole-dipole interactions, this dipole orientation would pass along the water chain. The water molecules near Na^+ suffer strong electrostatic interactions from Na^+, thus possessing strong dipole orientations. Those far away from Na^+ possess relative weak dipole orientations, and are easy to flip. When the two above opposite orientation effects meet together in the regions of gaps 1 and 7, H-bond defects were resulted. They are favorable to reduce the system energy by regulating the dipole orientations of the water chain on both sides. However, in the work of Zimmerli et al. [41], only "L-defect" was reported in the study of water transportation in a carbon nanotube. This is probably due to the structural difference between a carbon nanotube and a CPNT.

In addition, a test with a Cl^- positioned in the CPNT has been carried out. All the simulation conditions remain unchanged. The distributions of the dipole angles (θ) of water molecules in individual gaps have been investigated and the results are depicted in Fig. 13c, presenting strong dipole orientations of water molecules in each gap and no H-bond defects in the water chain. This is mainly due to the collaborative orientation effects of Cl^- and the carbonyl groups at the channel mouths.

Conclusions

Na^+ transportation through a transmembrane CPNT of $8×(WL)_4$ /POPE and its influences on water behaviors in the tube have been explored by molecular dynamics simulations. The PMF curve of a single Na^+ moving through the tube indicates that Na^+ possesses lower free energy in an α-plane region than in a mid-plane one. The non-bonding interactions of Na^+ with the CPNT, lipid and channel water indicate that the electrostatic interaction between Na^+ and channel water plays a determinant role in the fluctuation of the total non-bonding interaction energy. The distribution of the angles (θ) between the vectors of carbonyl groups (from O to C) and the tube axis (z) indicates that Na^+ can regulate the orientations of the carbonyl moieties at the tube mouths, which may be related with the unique selectivity of a CPNT to a cation.

Due to the spatial restriction of the CPNT channel, there are mainly two shells of water molecules around Na^+. The numbers of water molecules are 4.50 and 4.09 in the first solvation shell of Na^+, 3.10 and 4.08 in the second one for Na^+ locating in an α-plane zone and a mid-plane region, respectively. In the regions far away from Na^+, the density profile of water molecules proposes a wavelike pattern of water molecular distribution in the nanotube, suggesting that water molecules nearly arrange in a form of 1-2-1-2 file.

The introduction of Na^+ significantly influences the dipole orientations of water molecules in the tube. The dipole orientations of water molecules in gaps 2, 3, 5 and 6 all point to the opposite of Na^+ location. Nevertheless, water molecules in gaps 1 and 7 are forced to bear two contrary orientation effects from Na^+ and the carbonyl groups at the tube mouths, respectively. The most prominent feature of the joint effects is the formation of D-defects in water chain in gaps 1 and 7, which can accommodate energetically favorable water orientations in these regions.

References

1. Ghadiri MR, Granja JR, Milligan RA, McRee DE, Khazanovich N (1993) Self-assembling organic nanotubes based on a cyclic peptide architecture. Nature 366:324–327
2. Kim HS, Hartgerink JD, Reza Ghadiri M (1998) Oriented self-assembly of cyclic peptide nanotubes in lipid membranes. J Am Chem Soc 120:4417–4424

3. Hwang H, Schatz GC, Ratner MA (2009) Coarse-Grained molecular dynamics study of cyclic peptide nanotube insertion into a lipid bilayer. J Phys Chem A 113:4780–4787

4. Khalfa A, Treptow W, Maigret B, Tarek M (2009) Self assembly of peptides near or within membranes using coarse grained MD simulations. Chem Phys 358:161–170

5. Khurana E, DeVane RH, Kohlmeyer A, Klein ML (2008) Probing peptide nanotube self-assembly at a liquid-liquid interface with coarse-grained molecular dynamics. Nano Lett 8:3626–3630

6. Delemotte L, Dehez F, Treptow W, Tarek M (2008) Modeling membranes under a transmembrane potential. J Phys Chem B 112:5547–5550

7. Ghadiri MR, Granja JR, Buehler LK (1994) Artificial transmembrane ion channels from self-assembling peptide nanotubes. Nature 369:301–304

8. Jishi RA, Braier NC, White CT, Mintmire JW (1998) Peptide nanotubes: an inert environment. Phys Rev B 58:R16009–R16011

9. Liu J, Fan JF, Tang M, Cen M, Yan JF, Liu Z, Zhou WQ (2010) Water diffusion behaviors and transportation properties in transmembrane cyclic Hexa-, Octa- and decapeptide nanotubes. J Phys Chem B 114:12183–12192

10. Baumgaertner A (2009) Fast-ion transport in peptide nanochannels. Mat Sci Eng B 165:261–265

11. Liu J, Fan JF, Tang M, Zhou WQ (2010) Molecular dynamics simulation for the structure of the water chain in a transmembrane peptide nanotube. J Phys Chem A 114:2376–2383

12. Granja JR, Ghadiri MR (1994) Channel-mediated transport of glucose across lipid bilayers. J Am Chem Soc 116:10785–10786

13. Liu HF, Chen J, Shen Q, Fu W, Wu W (2010) Molecular insights on the cyclic peptide nanotube-mediated transportation of antitumor drug 5-Fluorouracil. Mol Pharm 7:1985–1994

14. Engels M, Bashford D, Reza Ghadiri M (1995) Structure and dynamics of self-assembling peptide nanotubes and the channel-mediated water organization and self-diffusion: a molecular dynamics study. J Am Chem Soc 117:9151–9158

15. Tarek M, Maigret B, Chipot C (2003) Molecular dynamics investigation of an oriented cyclic peptide nanotube in DMPC bilayers. Biophys J 85:2287–2298

16. García-Fandiño R, Granja JR, D'Abramo M, Orozco M (2009) Theoretical characterization of the dynamical behavior and transport properties of α, γ-peptide nanotubes in solution. J Am Chem Soc 131:15678–15686

17. Asthagiri D, Bashford D (2002) Continuum and atomistic modeling of ion partitioning into a peptide nanotube. Biophys J 82:1176–1189

18. Hwang H, Schatz GC, Ratner MA (2006) Steered molecular dynamics studies of the potential of mean force of a Na^+ or K^+ ion in a cyclic peptide nanotube. J Phys Chem B 110:26448–26460

19. Dehez F, Tarek M, Chipot C (2007) Energetics of ion transport in a peptide nanotube. J Phys Chem B 111:10633–10635

20. Choi K-M, Kwon CH, Kim HL, Hwang H (2012) Potential of mean force calculations for ion selectivity in a cyclic peptide nanotube. B Kor Chem Soc 33:911–916

21. Hilder TA, Gordon D, Chung S-H (2009) Boron nitride nanotubes selectively permeable to catons or anions. Small 5:2870–2875

22. Yang Y, Berrondo M, Henderson D, Busath D (2004) The importance of water molecules in ion channel simulations. J Phys-Condens Mat 16:S2145–S2148

23. Furini S, Beckstein O, Domene C (2009) Permeation of water through the KcsA K^+ channel. Proteins 74:437–448

24. Saparov SM, Pohl P (2004) Beyond the diffusion limit: water flow through the empty bacterial potassium channel. P Natl Acad Sci USA 101:480–4809

25. Brooks BR, Bruccoleri RE, Olafson BD, States DJ, Swaminathan S, Karplus M (1983) CHARMM: a program for macromolecular energy, minimization, and dynamics calculations. J Comput Chem 4:187–217

26. Jorgensen WL, Chandrasekhar J, Madura JD, Impey RW, Klein ML (1983) Comparison of simple potential functions for simulating liquid water. J Chem Phys 79:926–935

27. Martyna GJ, Tobias DJ, Klein ML (1994) Constant pressure molecular dynamics algorithms. J Chem Phys 101:4177–4189

28. York DM, Darden TA, Pedersen LG (1993) The effect of long-range electrostatic interactions in simulations of macromolecular crystals: a comparison of the Ewald and truncated list methods. J Chem Phys 99:8345–8348

29. Philips JC, Braun R, Wang W, Gumbart J, Tajkhorshid E, Villa E, Chipot C, Skeel RD, Kale L, Schulten K (2005) Scalable molecular dynamics with NAMD. J Comput Chem 26:1781–1802

30. Humphrey W, Dalke A, Schulten KJ (1996) VMD: visual molecular dynamics. Mol Graph 14:33–38

31. Bolhuis PG, Dellago C, Chandler D (2000) Reaction coordinates of biomolecular. P Natl Acad Sci USA 97:5877–5882

32. Cohen J, Schulten K (2004) Mechanism of anionic conduction across CIC. Biophys J 86:836–845

33. Sotomayor M, Schulten K (2007) Single-molecule experiments in vitro and in silico. Sience 316:1144–1148

34. Lee SH, Rasaiah JC (1996) Molecular dynamics simulation of ion mobility. 2. Alkali metal and halide ions using the SPC/E model for water at 25 °C. J Phys Chem 100:1420–1425

35. Park S, Khalili-Araghi F, Tajkhorshid E, Schulten K (2003) Free energy calculation from steered molecular dynamics simulations using Jarzynsk's equality. J Chem Phys 119:3559–3566

36. Okamoto H, Nakanishi T, Nagai Y, Kasahara M, Takeda K (2003) Variety of the molecular conformation in peptide nanorings and nanotubes. J Am Chem Soc 125:2756–2769

37. Obst S, Bradaczek H (1996) Molecular dynamics study of the structure and dynamics of the hydration shell of alkaline and alkaline-earth metal cations. J Phys Chem 100:15677–15687

38. Chang TM, Dang LX (1999) Detailed study of potassium solvaiton using molecular dynamics techniques. J Phys Chem B 103:4714–4720

39. Zhu FQ, Schulten K (2003) Water and proton conduction through carbon nanotubes as models for biological channels. Biophys J 85:236–244

40. Dellago C, Naor M, Hummer G (2003) Proton transport through water-filled carbon nanotubes. Phys Rev Lett 90:105902, 1−4

41. Zimmerli U, Gonnet PG, Walther JH, Koumoutsakos (2005) Curvature induced L-defects in water conduction in carbon nanotubes. Nano Lett 5:1017–1022